

One-dimensional and (001) Facetted Nanostructured TiO₂ Photoanodes for Dye-sensitized Solar Cells

Hong Lin*, Xiao Wang, and Feng Hao

Abstract: As one of the most important components in dye-sensitized solar cells (DSCs), photoanode materials have attracted massive interest and been greatly developed through the efforts of various research institutions in recent years. Photoanode materials not only provide a large surface for the sensitizer to favor charge separation, but also conduct the electrons to the collection electrode. In recent years, one-dimensional (1D) nanostructures (nanotubes (NT), nanowires (NW) and nanorods (NR)), which offer direct pathways for electron transport, and nanostructures (nanosheets (NS) and nanoparticles (NP)) with (001) crystal facets which possess higher surface energies have been widely employed as photoanode materials. In this review, the progress of 1D nanostructures and those with (001) crystal facets, as well as their photovoltaic performance in DSCs will be discussed briefly. Further efforts are needed to provide theoretical research for 1D and (001) facet nanostructured TiO₂ and to improve DSC performances based on these photoanodes.

Keywords: Dye-sensitized solar cells · (001) Facet · One-dimensional nanostructures · Photoanode materials · Titanium dioxide

1. Introduction

With low-cost, high theoretical power conversion efficiency and eco-friendly preparation techniques, dye-sensitized solar cells (DSCs) have attracted massive interest and been greatly developed through the efforts of various research institutions in recent years.^[1–7] During the initial stage, photoanode films of the DSCs were made up of sintered ZnO particles^[8,9] and textured TiO₂^[10] with rough surfaces, and the efficiencies of DSCs hovered at a level below 3% for a long time.^[11] The major reason for the low conversion efficiency was that the photoanode films could not provide enough surface area for sufficient dye adsorption to guarantee sufficient light harvesting. It has been reported that monolayers of dye molecules chemisorbed to the surface of the TiO₂ could enhance the conversion efficiency of DSCs. However, a further excess of dye was useless or even had an adverse effect on the photoelectrical process due to the lack of photoactivity and the filtering effect of the dye molecules not directly in contact with the semicon-

ductors. Therefore, it is imperative to find new ways to obtain a photoanode film with a large enough surface area for sufficient monolayer dye adsorption.^[10]

DSCs based on a mesoporous TiO₂ film made from nanocrystalline TiO₂ particles and organic sensitizers, were first reported by Prof. Grätzel in 1991.^[12] A typical DSC comprises conductive substrates as the collection electrode, an interconnected three-dimensional nanocrystalline film as photoanode formed from wide-bandgap semiconductors of inorganic oxides, sensitizers, an electrolyte and a counterelectrode. Unlike conventional solid-state semiconductor photovoltaics, DSCs accomplish the optical absorption and the charge separation processes by the association of the organic or inorganic sensitizer as light-absorbing material with the mesoporous or nanocrystalline film. Here, photoanode materials not only provide a large surface for the sensitizer to favor charge separation, but also conduct the electrons to the collection electrode. Therefore, photoanode materials play a very important role, and have become a hotspot of material chemistry research.^[13–16] Nanocrystalline TiO₂ particles as shown in Fig. 1,^[3] commonly used in DSCs these days, provide a large surface area (more than 1000 times larger than the projection surface^[17]) to ensure efficient dye loading and therefore improve light-harvesting performance.^[4] Moreover, the mesoporous TiO₂ nanoparticle (NP) film guarantees that the liquid electrolyte can permeate well into the interior of the film and form a good ohmic contact at the

interfaces between them, ensuring that the DSCs are working properly.

However, the observed diffusion coefficients of electrons in the TiO₂ NP film are two orders of magnitude lower than those in the bulk crystal, which can be roughly understood by the hypothesis of electron traps in the porous TiO₂ with a broad distribution.^[18,19] Defects in the porous TiO₂ may act as electron traps and exist in the grain boundaries between nanosized particles. To address these problems, various low-dimensional nanostructures have been proven to be effective alternatives to enhance the performance of DSCs due to their facilitated electron transport.

However, the TiO₂ NPs commonly applied in DSCs are much smaller than the wavelength of visible light. The film is thus transparent with little light scattering prop-

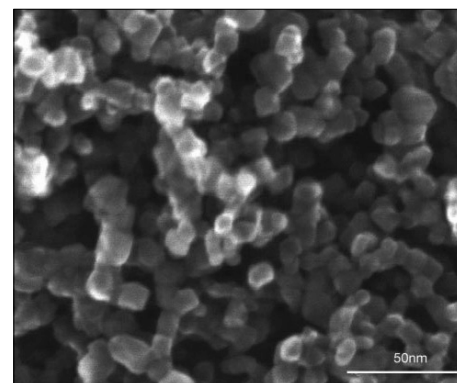


Fig. 1. SEM image of TiO₂ nanoparticle film. Reprinted with permission from Macmillan Publishers Ltd.: *Nature* 2001, 414, 338.

*Correspondence: Prof. Dr. H. Lin
State Key Laboratory of New Ceramics & Fine Processing
Department of Material Science and Engineering
Tsinghua University, China
Tel.: +86 62 772 672
E-mail: Hong-lin@tsinghua.edu.cn

erty. To address this problem, a variety of larger sized TiO_2 NPs (100 to 400 nm) has been widely employed as light-scattering centers to increase the optical length in the film, and an enhanced light-harvesting performance especially in the long wavelength region has been demonstrated both experimentally and theoretically.^[20–25] Besides these large sized nanoparticles, various one-dimensional (1D) nanostructures have also been shown to be effective alternatives to enhance the performance of DSCs due to their facilitated electron transport and enhanced light harvesting due to the light scattering effect.^[26–28]

In addition, nanostructured materials with tailored crystalline facets have recently attracted great interest arising from their unique geometrical and electronic structures such as high densities of atom steps, kinks, dangling bonds, and ledges.^[29–32] In the case of TiO_2 crystals, according to the principle of minimization of surface energy (0.90 J m^{-2} for the (001) facet $> 0.53 \text{ J m}^{-2}$ for the (100) facet $> 0.44 \text{ J m}^{-2}$ for the (101) facet), specific surfaces with high energy are usually eliminated during the crystal growth process.^[33] Under equilibrium conditions, natural and synthetic anatase TiO_2 single crystals mainly exist with a truncated octahedral bipyramid morphology, in which the majority of the surface is normally enclosed by energetically favorable (101) facets rather than the more reactive (001) facets.^[34] Very recently, the role of fluorine has attracted increased attention because of its capability to control particle morphology and facets of TiO_2 . With a much larger surface energy than (101) facets, (001) facets can form strong bonds with dye molecules, thus improving the dye adsorption and enhancing the performance of DSCs.^[35]

Based on the above discussion, a rational design of the photoanode structure to simultaneously enhance the light harvesting, electron transport and collection efficiency is of high priority for further efficiency enhancements. Recently, massive effort has been devoted to the 1D structure and (001) crystal facet structure for better electron transport performance, light scattering effect and dye adsorption. In this review, recent progress on the 1D structure (nanotubes and nanorods) which offer direct pathways for electron transport and nanosheets and nanoparticles with (001) crystal facets which have higher surface energies will be discussed.

2. 1D Nanostructures

In DSCs, photo-induced charge separation occurs by electron transport at the TiO_2 /dye/electrolyte interfaces, and the charges transfer in the TiO_2 matrix and

electrolyte separately.^[27] A further increase in conversion efficiency has been limited by energy loss due to recombination between electrons and either dye molecules or the oxidized electron-accepting species in the electrolyte during the charge transport process. 1D TiO_2 nanostructures such as nanotubes, nanowires, and nanorods have attracted considerable interest recently as they display unique electron transport characteristics and great potential to be applied in DSCs. Herein, recent progress with 1D TiO_2 nanostructures and their application in DSCs will be introduced.

2.1 Nanotubes

1D TiO_2 nanostructures, especially nanotubes (NTs), have been synthesized using various techniques such as anodization, sol-gel methods and template-based methods.

Anodization is a new technique to prepare oriented NTs arrays. Grimes first reported formation of uniform titania NTs arrays *via* anodic oxidation of titanium in a hydrofluoric electrolyte.^[36] To fabricate NTs arrays, titanium foil is firstly anodized to achieve ordered nanopores. These nanopores initially have an amorphous structure, which can be transformed to anatase TiO_2 upon annealing to over $450 \text{ }^\circ\text{C}$. Electrolyte composition and pH, determine both the rate of NTs array formation, as well as the rate of resultant oxide dissolution. In all cases, a fluoride ion-

containing electrolyte is required for NTs array formation. The dimensions of NTs can be precisely controlled by tailoring the electrochemical conditions. Uniform TiO_2 NTs arrays are easily grown with various pore sizes (22–110 nm), lengths (200 nm to $1000 \text{ }\mu\text{m}$), and wall thicknesses (7–34 nm).^[37] A typical morphology of TiO_2 NTs arrays is shown in Fig. 2.

The application of anodized TiO_2 NTs arrays on titanium foil as a photoanode material in DSCs was first reported in 2005.^[38] The configuration of this type of DSC is shown in Fig. 3. It has back-side illumination geometry since the titanium foil is non-transparent. An overall photo conversion efficiency (PCE) of 6.89% is achieved under standard illumination conditions (AM 1.5G, 100 mW/cm^2), with an open circuit voltage of 0.817 V, short circuit current density of 12.72 mA cm^{-2} , and fill factor of 0.663, while the photoelectrode film is comprised of $20 \text{ }\mu\text{m}$ long TiO_2 NTs.^[39]

The electronic transport dynamic of the 1D NTs electrodes was investigated by Frank and co-workers.^[40] As shown in Fig. 4, transport and recombination times for NTs- and NPs-based DSCs as a function of the incident photon flux (light intensity) were compared. The thicknesses of the NTs and NPs films (4.3 and $4.2 \text{ }\mu\text{m}$, respectively) in the cells were about the same, and the recombination time constants for the NTs arrays are an order of magnitude larger than those for the NPs films over the

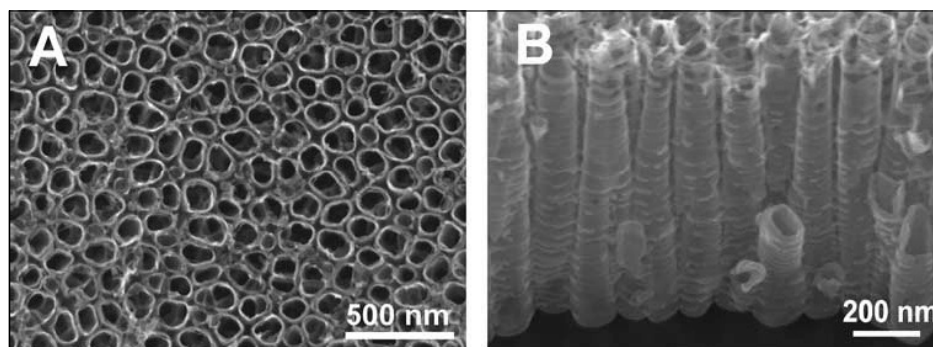


Fig. 2. Typical morphology of TiO_2 NTs arrays. Reprinted from *Electrochem. Commun.* **2005**, *7*, 1133 with permission of Elsevier.

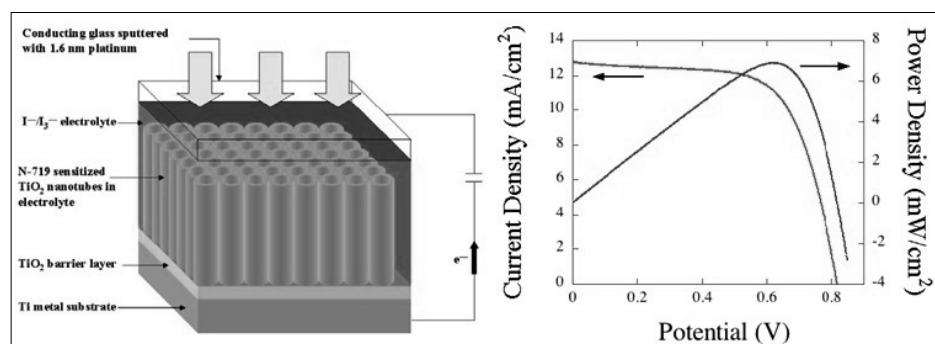


Fig. 3. Configuration of back-side illumination geometry DSCs and its I-V characteristics plots. Reprinted from *Nanotechnology* **2007**, *18*, 65707 with permission of IOP.

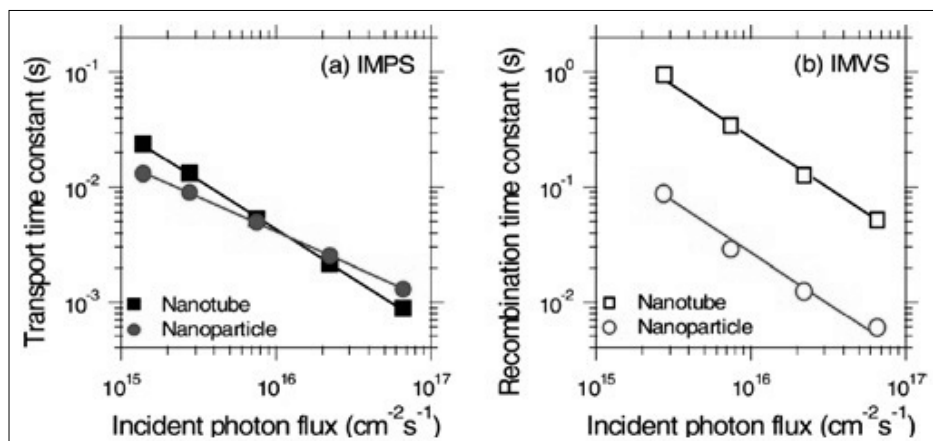


Fig. 4. Comparison of (a) transport and (b) recombination time constants for NTs- and NPs-based DSCs as a function of the incident photon flux for 680 nm laser illumination. Reprinted with permission from *Nano Lett.* **2007**, 7, 69. Copyright 2007 American Chemical Society.

light-intensity range investigated, resulting in a large charge collection efficiency (25% larger than that for the NPs films) for NTs electrodes. The slower recombination could indicate that fewer potential surface recombination sites exist in NTs arrays than in NPs films. Therefore, the NTs films can be made thicker than NPs films for a higher light-harvesting efficiency.

The application of TiO₂ NTs grown on Ti-foil requires back-side illumination, which is not the optimal configuration for DSCs because the platinum counterelectrode partially reflects light and the iodine in the electrolyte absorbs photons in the near UV region.^[41] To resolve this problem, Park *et al.*^[42] described a simple and inexpensive transfer methodology. The highly-ordered, 7~35 μm-thick TiO₂ was transferred onto fluorine-doped tin oxide (FTO) glass, with two drops of 100 mM Ti-isopropoxide to form interconnections between the FTO glass and the TiO₂ film. Under standard illumination conditions (AM 1.5G, 100 mW/cm²), the NTs-based DSCs with 35 μm-thick TiO₂ NTs arrays exhibited a short-circuit current of 16.8 mA cm⁻², an open-circuit voltage of 0.733 V and a fill factor of 62%, with a PCE of 7.6%.

2.2 Nanowires

In DSCs, a single crystalline and topologically ordered photoanode could provide direct electrical pathways for photogenerated electrons and enhance the electron transport rate. Therefore, oriented NW and NR arrays could also be of benefit to such photovoltaic devices. Here the hydrothermal process is discussed, which offers potential for large-scale and low-cost production and precise control of the nanostructures.

Lin and co-workers reported the photovoltaic performance of DSCs using TiO₂ NWs arrays synthesized by a hydrothermal

process.^[43] Titanate (Na₂Ti₅O₁₁) NWs arrays were grown vertically on metal titanium (Ti) substrates using a three-step synthesis method. Then, the Na₂Ti₅O₁₁ NWs array film was immersed into an HCl aqueous solution to exchange Na⁺ for H⁺. The resulting hydrogen titanate (H₂Ti₅O₁₁·H₂O) NWs array film was postannealed at 450 °C for 2 h and transformed into a TiO₂ NW array film, which still retained the intact structure (Fig. 5). The NW thin film was shed from the substrate as a membrane, pasted onto a conductive glass and

assembled into a DSC. A PCE of 6.58% for the DSC was obtained, which was 16% higher than that of the DSC prepared using commercial TiO₂ powder (P25) with nearly the same thickness.

3. Hybrid Nanostructures of 1D Nanostructures Mixed with Nanoparticles

Based on the discussion above, 1D nanostructured TiO₂ materials have shown excellent performance on electron transport. However, the performance of most 1D nanostructured TiO₂ materials-based DSCs were not as high as expected due to the limited surface area. To solve this problem, researchers tried to construct composite photoanodes by mixing 1D nanostructured TiO₂ materials and TiO₂ NPs. Lin and co-workers reported that a commercial P25 nanoparticle photoanode film decorated with rutile NRs exhibited an outstanding performance in DSCs.^[28] The TiO₂ NRs were obtained through a facile acidic hydrothermal method, and determined to be single crystals as shown in Fig. 6. The performance of NR-decorated P25 devices was much better than the blank P25 devices, which was especially reflected in their magnitude of J_{sc} , which was ascribed to the light scattering and fast electronic transport of the TiO₂ NRs.

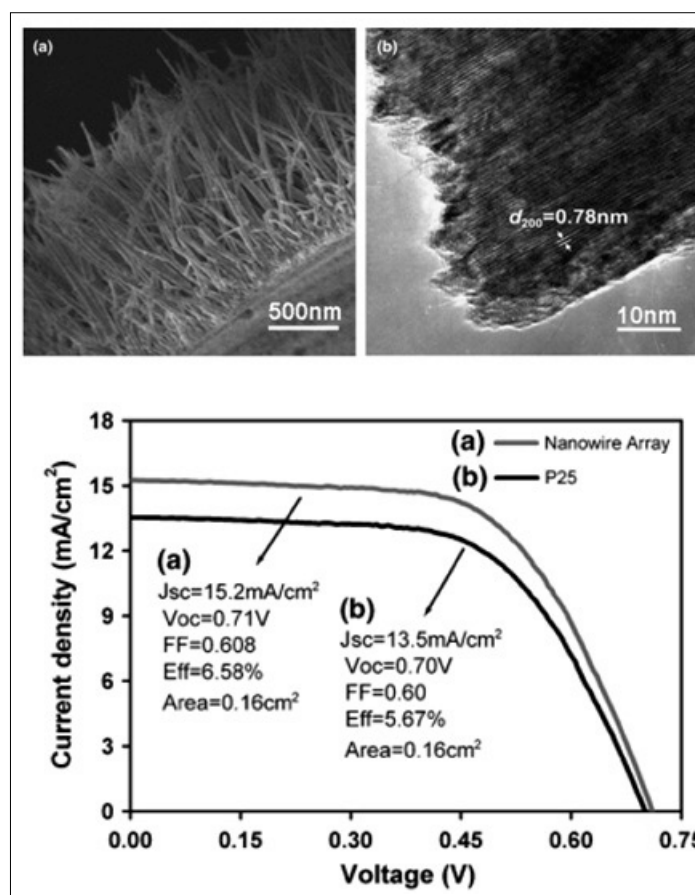


Fig. 5. Typical morphology of TiO₂NWs arrays and its I-V characteristics plots. Reprinted with permission from *J. Am. Ceram. Soc.* **2008**, 91, 628. Copyright 2008, John Wiley & Sons, Inc.

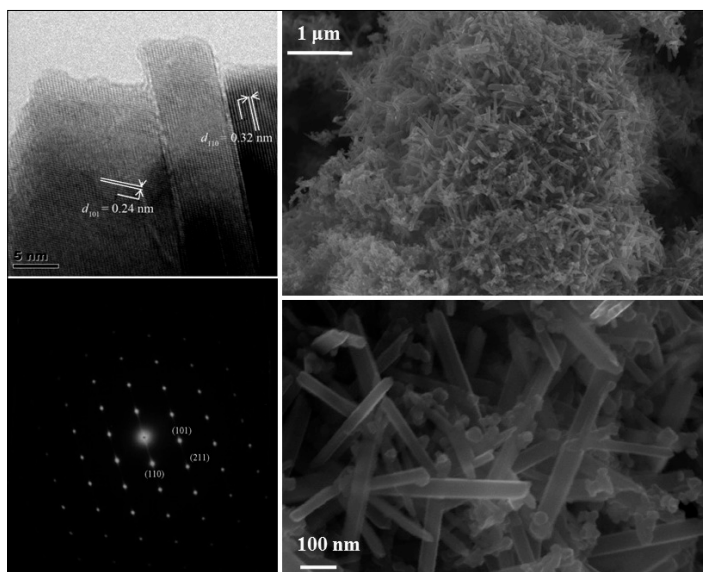


Fig. 6. FESEM and HRTEM images of the as-prepared TiO_2 nanocomposite at different magnifications and the corresponding SAED pattern of the NRs. Reproduced with permission of the PCCP Owner Societies. *Phys. Chem. Phys. Chem.* **2011**, *13*, 15918.

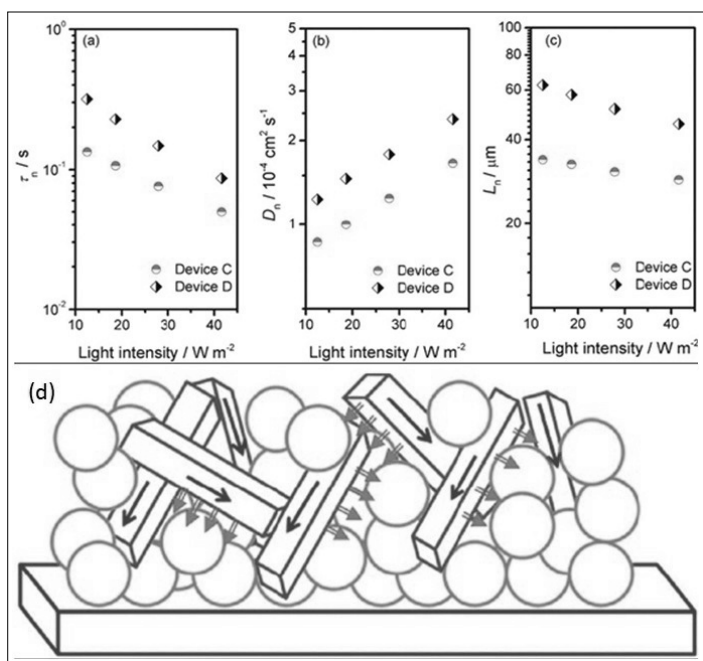


Fig. 7. Plots of electron lifetime (a), effective electron diffusion coefficient (b), and electron diffusion length (c) in DSCs based on TiO_2 NRs mixed with P25 and blank P25 from IMVS/IMPS measurements, and schematic diagram of dual benefits of the single-crystalline NRs decorated composite photoanode (d). Reproduced with permission of the PCCP Owner Societies. *Phys. Chem. Phys. Chem.* **2011**, *13*, 15918.

As presented in Fig. 7, intensity-modulated photocurrent/photovoltage spectra (IMPS/IMVS) measurements were used to gain information into the kinetic electron transport and recombination processes. Notably, introduction of the single-crystalline rutile NRs in the P25 matrix could simultaneously enhance the electron lifetimes and electron diffusion coefficient of the device compared to the blank P25 device. It is reasonable that the TiO_2 NRs played a role of a ‘highway’ for electron transport, which could improve the electron transfer rate, thus reduce the charge recombination. On the other hand, it is evident that NR-decorated P25 devices show a light scattering effect, as demonstrated in Fig. 7, where the arrows in grey represent the light scattering effect of the incorporated single-crystalline NRs.

4. Nanosheets and Nanoparticles with (001) Crystal Facets

In 2008, Yang and co-workers first successfully synthesized uniform anatase TiO_2 single crystals with a high percentage (47–64%) of (001) facets using hydrofluoric acid as a morphology controlling agent.^[44,45] In this work, a systematic investigation was carried out with various adsorption atoms to change the relative stabilities of (101) and (001) crystal facets based on first-principle calculations, and the authors discovered that F atoms not only yielded the lowest value of surface energy for both the (001) and (101) surfaces, but also resulted in (001) surfaces that were more stable than (101) surfaces. Based on this theoretical prediction, titanium tetrafluoride (TiF_4) aqueous

solution and hydrofluoric acid were used as an anatase single crystal precursor and crystal growth controlling agent, and TiO_2 nanosheets with a high percentage of (001) crystal facets were obtained as shown in Fig. 8.

Despite progress in the practical applications of anatase TiO_2 containing predominantly highly reactive (001) facets in photocatalytic materials and devices, there are very few studies focusing on the performance of DSCs fabricated with nano-sized anatase TiO_2 single crystals with high-energetic facets. Yu *et al.* reported an improved PCE for a DSC fabricated with anatase TiO_2 nanosheets (NSs) with exposed (001) facets (4.56%) compared to a DSC fabricated with traditional P25 nanoparticles (3.64%).^[46] The NSs were 70–80 nm in size, and only 8 nm thick, and the J_{sc} of the TiO_2 NSs based cell was much higher than that of the P25, which is mainly due to their enhanced light scattering properties as shown by UV-VIS diffuse reflectance spectra.

Recently, Wu *et al.* reported that with an increased percentage of exposed (001) facets (10%, 38%, and 80% as NSCT-c, NSCT-b and NSCT-a respectively), the PCE increased sequentially (7.47%, 8.14% to 8.49%).^[35] In this work, the surface areas of the as-prepared samples NSCT-a, and NSCT-b were determined to be similar (89.2 m^2/g and 91.4 m^2/g), while the dye loading of NSCT-a ($0.95 \times 10^{-7} \text{mol cm}^{-2}$) was larger than that of NSCT-b ($0.84 \times 10^{-7} \text{mol cm}^{-2}$), which means that exposed (001) facets in the TiO_2 play a very important role in determining the dye adsorption capability of the photoanode.

The dye loading capacity of nanocrystals with high-energetic (001) facets was further studied by Lin and co-workers.^[47] Nanoparticles with (001) crystal facets which had a similar surface area (46.50 m^2/g) to P25 nanoparticles (50.08 m^2/g) were obtained through a green hydrothermal method in which ammonium fluoride

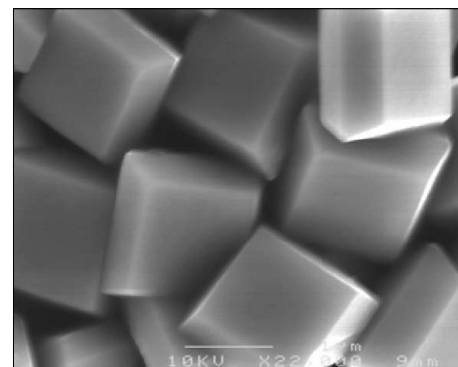


Fig. 8. Typical morphology of TiO_2 NSs with (001) crystal facets. Reprinted with permission from Macmillan Publishers Ltd.: *Nature* **2008**, *453*, 638.

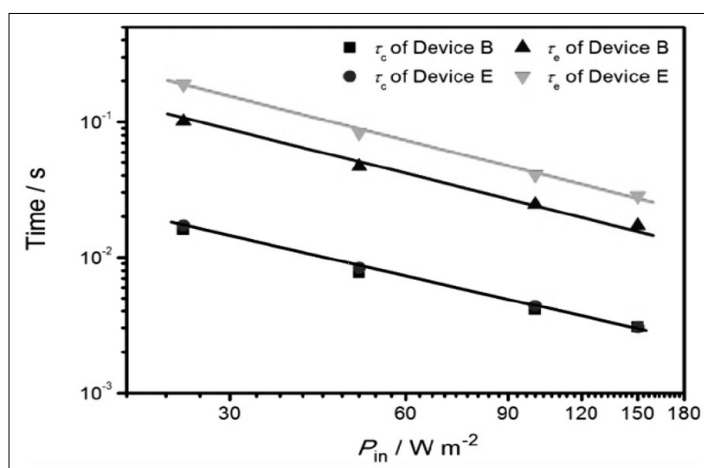


Fig. 9. Plots of effective electron lifetime (τ_e) and electron collection time (τ_c) in DSCs based on P25 and nanoparticles with (001) crystal facet from IMVS/IMPS measurements under various incident light intensities. Reprinted with permission from *J. Phys. Chem. C* **2012**, *116*, 19164. Copyright 2012 American Chemical Society.

(NH₄F) was used as shape-capping reagent. Unexpectedly the derived dye-loadings of the two different kinds of photoanodes were quite different, $6.74 \times 10^{-5} \text{ mol g}^{-1}$ for the P25 photoanode and $7.91 \times 10^{-5} \text{ mol g}^{-1}$ for the (001)-faceted single crystal photoanode, demonstrating a 17% enhancement of the dye-loading capacity for the (001)-faceted electrode. According to previous studies, the anatase (001) surfaces with high surface energy have a strong ability to absorb a (COOH) group.^[48,49] During this process, the carbonyl O atom binds to 5-fold-coordinated Ti atoms (Ti_{5c}) on the (001) surfaces, while the hydroxyl is transferred to 2-fold-coordinated O atoms (O_{2c}).^[50] Moreover, on the basis of the *ab initio* density-functional computation, the densities of the 5-fold-coordinated Ti atoms on the (101) and (001) facets were 5.1×10^{-2} and $7.0 \times 10^{-2} \text{ \AA}^{-2}$, respectively.^[51] This might be the primary reason for the notably enhanced dye-loading of the electrode with the exposed (001) facets. Moreover, as shown in Fig. 9, it was confirmed that incorporation of the (001)-faceted single crystalline nanoparticles into the working electrode had little influence on the electron collection time (τ_c); however, as compared with the P25-based device, the electron lifetime (τ) in the device with (001) faceted single crystalline nanoparticles was increased by almost 2-fold in magnitude, which was mainly ascribed to the different surface configuration in the single crystals exposed with high energetic (001) facets, such as plentiful dangling bonds and surface defects.

However, Kavan *et al.* reported that the anatase (001) facets adsorbed a smaller amount of sensitizer (C101) per unit area than the (101) facet,^[52] while an enhancement of Voc was achieved for (001) faceted DSCs which was due to the negative shift of the flatband. In addition, Pan *et al.* concluded that the conduction band edge of (001) facet was upshifted.^[53] Therefore, further theoretical and experimental re-

search is needed for a better understanding of the high energy facets of the photoanodes in DSC.

5. Conclusions and Outlook

The nanostructured TiO₂ materials for photoanodes in DSCs have undergone a great development in recent years, and various morphology systems have been developed in the search for superior electron transport kinetics and better photovoltaic performance. The requirements of an ideal photoanode material for highly efficient DSCs are mainly reflected in the following aspects: i) high specific surface area to ensure sufficient dye adsorption capacity; ii) directional structure to improve electron transport, and reduce the energy loss caused by charge recombination; iii) light scattering caused by the larger size nanostructured assemblies to increase the optical length in the photoanode film; iv) high energy surfaces such as anatase (001) facets to form a strong bond with dye molecules, thus improving the dye adsorption.

At present, 1D structures (nanotubes, nanowires and nanorods), as well as nanosheets and nanoparticles with (001) crystal facets display good performance when incorporated into DSCs. 1D structures show an obvious advantage in the electron transport and a certain light scattering effect when mixed with nanoparticles. Nanosheets and nanoparticles with high energy (001) crystal facets have become a hot topic in the past few years stemming from their unique electronic structures. These high-energetic facet-based nanocrystals can form a strong bond with dye molecules and thus improve dye adsorption. Further efforts are needed to provide a theoretical basis for 1D and (001) faceted nanostructured TiO₂ and to improve DSC performances based on these photoanodes.

Acknowledgements

Financial support from the National High Technology Research and Development Program of China (863 Program, 2006AA03Z218, 2011AA050522), the International Cooperation S&T Cooperation Program of China (2010DFA64360), and the National Natural Science Foundation of China (NSFC, 50672041) is greatly appreciated.

Received: January 23, 2013

Revised: February 23, 2013

- [1] M. Grätzel, *Acc. Chem. Res.* **2009**, *42*, 1788.
- [2] A. Hagfeldt, G. Boschloo, L. Sun, L. Kloo, H. Pettersson, *Chem. Rev.* **2010**, *110*, 6595.
- [3] M. Grätzel, *Nature* **2001**, *414*, 338.
- [4] I. Robel, V. Subramanian, M. Kuno, P. V. Kamat, *J. Am. Chem. Soc.* **2006**, *128*, 2385.
- [5] M. Grätzel, *J. Photochem. Photobiol. C* **2003**, *4*, 145.
- [6] A. Hagfeldt, M. Grätzel, *Chem. Rev.* **1995**, *95*, 49.
- [7] D. Zhao, T. Y. Peng, L. L. Lu, P. Cai, P. Jiang, Z. Q. Bian, *J. Phys. Chem. C* **2008**, *112*, 8486.
- [8] N. Alonso, M. Beley, P. Chartier, V. Ern, *Rev. Phys. Appl.* **1981**, *16*, 5.
- [9] M. Matsumura, Y. Nomura, H. Tsubomura, *Bull. Chem. Soc. Jpn.* **1977**, *50*, 2533.
- [10] M. Nazeeruddin, P. Liska, J. Moser, N. Vlachopoulos, M. Grätzel, *Helv. Chim. Acta* **1990**, *73*, 1788.
- [11] Q. F. Zhang, G. Z. Cao, *Nano Today* **2011**, *6*, 91.
- [12] B. O'Regan, M. Grätzel, *Nature* **1991**, *353*, 737.
- [13] Y. Kondo, H. Yoshikawa, K. Awaga, M. Murayama, T. Mori, K. Sunada, S. Bandow, S. Iijima, *Langmuir* **2008**, *24*, 547.
- [14] H. G. Yang, C. H. Sun, S. Z. Qiao, J. Zou, G. Liu, S. C. Smith, H. M. Cheng, G. Q. Lu, *Nature* **2008**, *453*, 638.
- [15] X. Han, Q. Kuang, M. Jin, Z. Xie, L. Zheng, *J. Am. Chem. Soc.* **2009**, *131*, 3152.
- [16] A. Ghicov, P. Schmuki, *Chem. Commun.* **2009**, 2791.
- [17] C. J. Barbé, F. Arendse, P. Comte, M. Jirousek, F. Lenzmann, V. Shklover, M. Grätzel, *J. Am. Ceram. Soc.* **1997**, *80*, 3157.
- [18] A. C. Fisher, L. M. Peter, E. A. Ponomarev, A. B. Walker, K. G. U. Wijayantha, *J. Phys. Chem. B* **2000**, *104*, 949.
- [19] A. Solbrand, A. Henningson, S. Sodergren, H. Lindström, A. Hagfeldt, S. E. Lindquist, *J. Phys. Chem. B* **1999**, *103*, 1078.
- [20] A. Usami, *Chem. Phys. Lett.* **1997**, *277*, 105.
- [21] J. Ferber, J. Luther, *Sol. Energy Mater. Sol. Cells* **1998**, *54*, 265.
- [22] G. Rothenberger, P. Comte, M. Grätzel, *Sol. Energy Mater. Sol. Cells* **1999**, *58*, 321.
- [23] J. Yu, J. Fan, K. Lv, *Nanoscale* **2010**, *2*, 2144.
- [24] M. K. Nazeeruddin, R. Splivallo, P. Liska, P. Comte, M. Grätzel, *Chem. Commun.* **2003**, 1456.
- [25] B. Tan, Y. Y. Wu, *J. Phys. Chem. B* **2006**, *110*, 15932.
- [26] M. Law, L. E. Greene, J. C. Johnson, R. Saykally, P. Yang, *Nat. Mater.* **2005**, *4*, 455.
- [27] J. Jiu, S. Isoda, F. Wang, M. Adachi, *J. Phys. Chem. B* **2006**, *110*, 2087.
- [28] F. Hao, H. Lin, C. Zhou, Y. Liu, J. Li, *Phys. Chem. Chem. Phys.* **2011**, *13*, 15918.
- [29] A. S. Barnard, L. A. Curtiss, *Nano Lett.* **2005**, *5*, 1261.
- [30] N. Tian, Z. Y. Zhou, S. G. Sun, Y. Ding, Z. L. Wang, *Science* **2007**, *316*, 732.
- [31] X. Han, M. Jin, S. Xie, Q. Kuang, Z. Jiang, Y. Jiang, Z. Xie, L. Zheng, *Angew. Chem. Int. Ed.* **2009**, *48*, 9180.
- [32] B. H. Wu, C. Y. Guo, N. F. Zheng, Z. X. Xie, G. D. Stucky, *J. Am. Chem. Soc.* **2008**, *130*, 17563.

- [33] M. Lazzeri, A. Selloni, *Phys. Rev. Lett.* **2001**, 87, 266105.
- [34] A. S. Barnard, L. A. Curtiss, *Nano Lett.* **2005**, 5, 1261.
- [35] X. Wu, Z. G. Chen, G. Q. Lu, L. Z. Wang, *Adv. Funct. Mater.* **2011**, 21, 4167.
- [36] C. A. Grimes, *Sol. Energy Mater. Sol. Cells* **2006**, 90, 2011.
- [37] K. Shankar, J. I. Basham, N. K. Allam, O. K. Varghese, G. K. Mor, X. Feng, M. Paulose, J. A. Seabold, K. Choi, C. A. Grimes, *J. Phys. Chem. C* **2009**, 113, 6327.
- [38] J.M. Macak, H. Tsuchiya, A. Ghicov, P. Schmuki, *Electrochem. Commun.* **2005**, 7, 1133.
- [39] K. Shankar, G. K. Mor, H. E. Prakasam, S. Yoriya, M. Paulose, O. K. Varghese, C. A. Grimes, *Nanotechnology* **2007**, 18, 65707.
- [40] K. Zhu, N. R. Neale, A. Miedaner, A. J. Frank, *Nano Lett.* **2007**, 7, 69.
- [41] K. Yu, J. Chen, *Nanoscale Res. Lett.* **2009**, 4, 1.
- [42] J. H. Park, T. Leeb, M. G. Kang, *Chem. Commun.* **2008**, 25, 2867.
- [43] W. L. Wang, H. Lin, J. B. Li, N. Wang, *J. Am. Ceram. Soc.* **2008**, 91, 628.
- [44] H. G. Yang, C. H. Sun, S. Z. Qiao, J. Zou, G. Liu, S. C. Smith, H. M. Cheng, G. Q. Lu, *Nature* **2008**, 453, 638.
- [45] H. G. Yang, G. Liu, S. Z. Qiao, C. H. Sun, Y. G. Jin, S. C. Smith, J. Zou, H. M. Cheng, G. Q. Lu, *J. Am. Chem. Soc.* **2009**, 131, 4078.
- [46] J. G. Yu, J. J. Fan, K. L. Lv, *Nanoscale* **2010**, 2, 2144.
- [47] F. Hao, X. Wang, C. Zhou, X. J. Jiao, X. Li, J. B. Li, H. Lin, *J. Phys. Chem. C* **2012**, 116, 19164.
- [48] X. Q. Gong, A. Selloni, *J. Phys. Chem. B* **2005**, 109, 19560.
- [49] A. Selloni, *Nat. Mater.* **2008**, 7, 613.
- [50] X. G. Gong, A. Selloni, A. Vittadini, *J. Phys. Chem. B* **2006**, 110, 2804.
- [51] M. Lazzeri, A. Vittadini, A. Selloni, *Phys. Rev. B* **2001**, 63, 15.
- [52] B. Laskova, M. Zikalova, L. Kavan, A. Chou, P. Liska, Z. Wei, L. Bin, P. Kubat, E. Ghadiri, J. E. Moser, M. Grätzel, *J. Solid State Electrochem.* **2012**, 16, 2993.
- [53] J. Pan, G. Liu, G. Q. Lu, H. M. Cheng, *Angew. Chem. Int. Ed.* **2011**, 50, 2133.